

TABLE 2.2. - Relation between different even polarization parameters of spin 1 particle

<p>(a) Even part of the density matrix for spin 1 particle</p> $\rho = \begin{vmatrix} \rho_{11} & \rho_{10} & \rho_{1-1} \\ \bar{\rho}_{10} & \rho_{00} & -\bar{\rho}_{10} \\ \bar{\rho}_{1-1} & -\bar{\rho}_{10} & \rho_{11} \end{vmatrix} \quad \rho_{00} = 1 - 2\rho_{11}$	
<p>(b) Relation between the matrix elements in (a) and the multipole parameters in Table 2.1.</p> $\begin{array}{l l} r_0^{(2)} = \rho_{11} - \rho_{00} & \text{(BH)} \\ r_2^{(2)} = \sqrt{3} \operatorname{Re} \rho_{1-1} & r_{-2}^{(2)} = -\sqrt{3} \operatorname{Im} \rho_{1-1} \\ \hline \text{(BT)} \quad r_1^{(2)} = \sqrt{6} \operatorname{Re} \rho_{10} & r_{-1}^{(2)} = -\sqrt{6} \operatorname{Im} \rho_{10} \end{array}$	
<p>(c) Relation between the multipole parameters for transversity and helicity quantizations</p> $\begin{array}{l l} H_{r_0}^{(2)} = -\sqrt{\frac{1}{4}} T_{r_0}^{(2)} - \sqrt{\frac{3}{4}} T_{r_2}^{(2)} & \text{(B)} \\ H_{r_2}^{(2)} = -\sqrt{\frac{3}{4}} T_{r_0}^{(2)} + \sqrt{\frac{1}{4}} T_{r_2}^{(2)} & H_{r_{-2}}^{(2)} = T_{r_1}^{(2)} \\ H_{r_1}^{(2)} = -T_{r_{-2}}^{(2)} & H_{r_{-1}}^{(2)} = -T_{r_{-1}}^{(2)} \end{array}$	
<p>(d) Relation between the multipole parameters for two different transversity quantizations (rotation on the normal of angle ϕ_{ba})</p> $\begin{array}{l} T_{b r_0}^{(2)} = T_{a r_0}^{(2)} \\ T_{b r_M}^{(2)} = \cos(M\phi_{ba}) T_{a r_M}^{(2)} - \sin(M\phi_{ba}) T_{a r_{-M}}^{(2)} \\ T_{b r_{-M}}^{(2)} = \sin(M\phi_{ba}) T_{a r_M}^{(2)} + \cos(M\phi_{ba}) T_{a r_{-M}}^{(2)} \end{array} \quad \begin{array}{l} M = 1, 2 \\ \text{(B2)} \end{array}$	

(BH) For B-symmetry and helicity quantization, the parameters in this column are zero.

(BT) For B-symmetry and transversity quantization, the parameters in this line are zero.

(B) For B-symmetry, the parameters in this column are zero.

(B2) For B-symmetry, $M = 2$.

2.3. Polarization domain for B-symmetric spin 1 particle.

The domain of possible values of the three even polarization parameters of a B-symmetric spin 1 particle is fixed by the requirement that the full density matrix, including eventually some ghost parameters, must be positive, i. e., the probabilities of the different pure states present in the statistical mixture must be positive (cf. I. A. 6).

This "polarization domain" can be studied intrinsically, i. e., independently of any concrete system of parametrization. It is a truncated cone. Furthermore, for the conveniently normalized intrinsic metric of the matrix space, this polarization domain is a "equilateral cone" which can be inscribed in a unitary sphere, i. e., each meridian plane cut them along a equilateral triangle which can be inscribed in a circle of radius 1 (see Fig. 2.1). The unpolarized state is represented by the center of this sphere, O . The distance of any representative point to this "isotropy center" gives directly the degree of even polarization of the corresponding state. Therefore the only even pure states are represented by the vertex of the cone and the circumference of its base. The vertex, P_3 , represents the pure state with polarization vector directed along the normal (in other words, a pure state whose magnetic quantum number is zero for a quantization along the normal, a pure state that in some usual terminology will be called longitudinally polarized, or simply, polarized along the normal). Any point of the circumference of the base represents a pure state with polarization vector in some real direction inside of the production three-plane, so that two diametrically opposite points, like P_1 and P_2 , correspond to two orthogonal directions of polarization. (Remark that pure states with polarization vector along a non-real direction, like the pure states with magnetic quantum number $+1$ or -1 , are not even, and that pure states with polarization vector along a real direction outside of the normal and the production three-plane are not B-symmetric).

Any representative point inside this truncated cone can be intrinsically interpreted in the following way. It will be contained at least in one of the meridian sections of the cone. Therefore it will represent a mixture of the three pure states represented by the vertices of the equilateral triangle, i. e., three pure states with polarization vector along three orthogonal directions. If the probabilities of these three pure states are materialized by weights at the

vertices of the triangle, the point representative of the mixture is their bary-center. (Equivalently, these three probabilities are proportional to the triangular coordinates of the representative point, the proportionality coefficient being 2/3).

A concrete frame of quantization will allow to fix a basis for the polarization parameters, and to write down the inequalities defining this polarization domain. Table 2.3. gives the inequalities and Fig. 2.1. indicates the axes of the normalized multipole parameters, $r_M^{(2)}$, for any pair of associated transversity and helicity frames of quantization. As shown by the relations of Table 2.2 (c), they are related through a rotation of π radians around the axis a .

If the quantization frames are rotated by an angle ψ_{ba} around the normal, according to Table 2.2 (d), the parameter axes of Fig. 2.1 are in turn rotated by an angle $2 \cdot \psi_{ba}$ around the symmetry axis of the cone. (Thus, P_1 , P_2 and P_3 represent the pure states with polarization vector along the axes x , y , and z of the chosen transversity frame).

Therefore, any such rotations leave invariant the polarization parameters $T_{r_o}^{(2)}$ and $T_{r_{p_2}}^{(2)} = \sqrt{[T_{r_2}^{(2)}]^2 + [T_{r_{-2}}^{(2)}]^2}$. Thus, a convenient two dimensional representation of the points inside the cone, that displays their cylindrical coordinates, is proposed in Fig. 2.2. Its diagram a) presents these two polarization parameters which are invariant under rotations of the quantization axis around the normal. In this diagram, the representative points must be the same for measurements corresponding to s, t or u frames of quantization. The positivity conditions require that the points be inside the half equilateral triangle. Their distance to the origin O shows directly the degree of even polarization. On the other hand, the diagram b) of Fig. 2.2 giving the angle of these cylindrical coordinates $T_{r_{\vartheta_2}}^{(2)}$, depends completely on the chosen transversity parametrization. Because of this it would be worthwhile to measure and to draw this diagram for s, t and u frames of quantization.

For t frame of quantization this parametrization is equivalent to the parametrization supplied by the so called "dynamic reference system" (cf. Donohue and Høgaasen, 67). This system is obtained from the t -helicity frame by means of a rotation around the normal by so an angle Θ , that the double rotation of the polarization axes will place a given polarization point inside the triangle $P_1 P_2 P_3$ of Fig 2.1. (and inside its right half). Therefore our $T_{r_{\vartheta_2}}^{(2)} = 2 \Theta$. Instead our rectangular coordinates $T_{r_{p_2}}^{(2)}$ and $T_{r_o}^{(2)}$ they

propose the triangular coordinates α , β , and γ (with $\alpha + \beta + \gamma = 1$), which give the probabilities of the pure states P_1 , P_3 and P_2 .

Instead of these normalized multipole parameters one could use the density matrix elements, let us say ρ_{11} , $\text{Re } \rho_{1-1}$ and $\text{Im } \rho_{1-1}$ for transversity, and ρ_{11} , $\text{Re } \rho_{1-1}$ and $\text{Re } \rho_{10}$ for helicity quantization (so, e.g., Gottfried and Jackson, 64, for t-helicity quantization). According to Table 2.2 (a) and (b), the transversity and helicity axes represented in Fig. 2.1, will be translated to the points P_3 and P_2 respectively, and for these new axes different scale factors in the different directions have to be introduced, if we want to keep the intrinsic metric of the figure. This has been shown in Fig. 2.3.

Remark that in Fig. 2.1 and Fig. 2.2 only the three measurable parameters of a B-symmetric density matrix are represented. If the ghost parameter, $T_{r_0}^{(1)}$, would be added, the corresponding positivity domain would be an analogous truncated cone but with three dimensions orthogonal to the revolution axis. Because of that, for instance, any point inside the base of the cone in Fig. 2.1 can represent the projection of two B-symmetric pure states with partially even and partially odd polarization.

TABLE 2.3. - Positivity conditions for the measurable polarization parameters of B-symmetric spin 1 particle

(a) Positivity conditions for transversity parametrization

$$-1 < T_{r0}^{(2)} < \frac{1}{2}$$

$$[T_{r2}^{(2)}]^2 + [T_{r-2}^{(2)}]^2 < \frac{1}{3}[T_{r0}^{(2)} + 1]^2$$

(b) Positivity conditions for helicity parametrization

$$-\sqrt{\frac{1}{3}}[H_{r0}^{(2)} + 1] < H_{r2}^{(2)} < \sqrt{\frac{1}{3}}[H_{r0}^{(2)} + 1]$$

$$|H_{r1}^{(2)}| < \frac{1}{3}[1 - 2H_{r0}^{(2)}][1 + H_{r0}^{(2)} - \sqrt{3}H_{r2}^{(2)}]$$

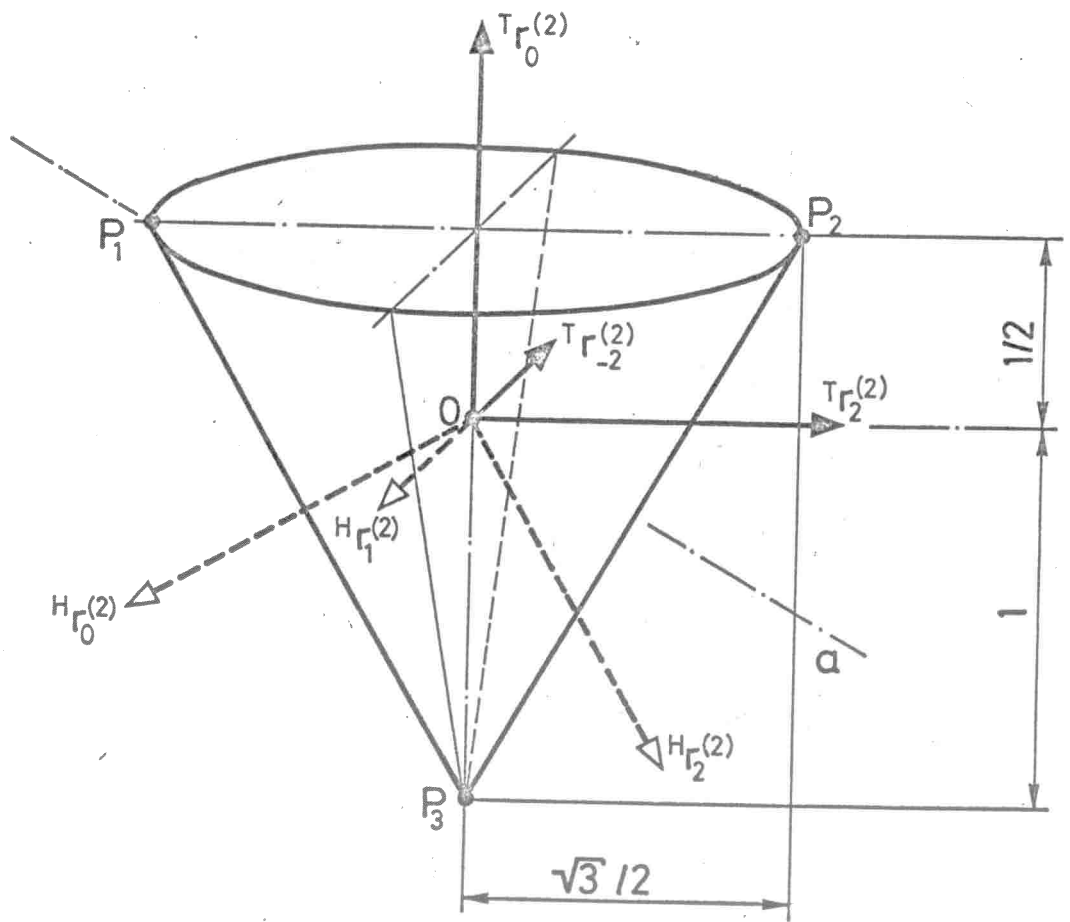


FIG. 2.1

FIG. 2.1. Domain of the even, B-symmetric polarization of spin 1 particle.

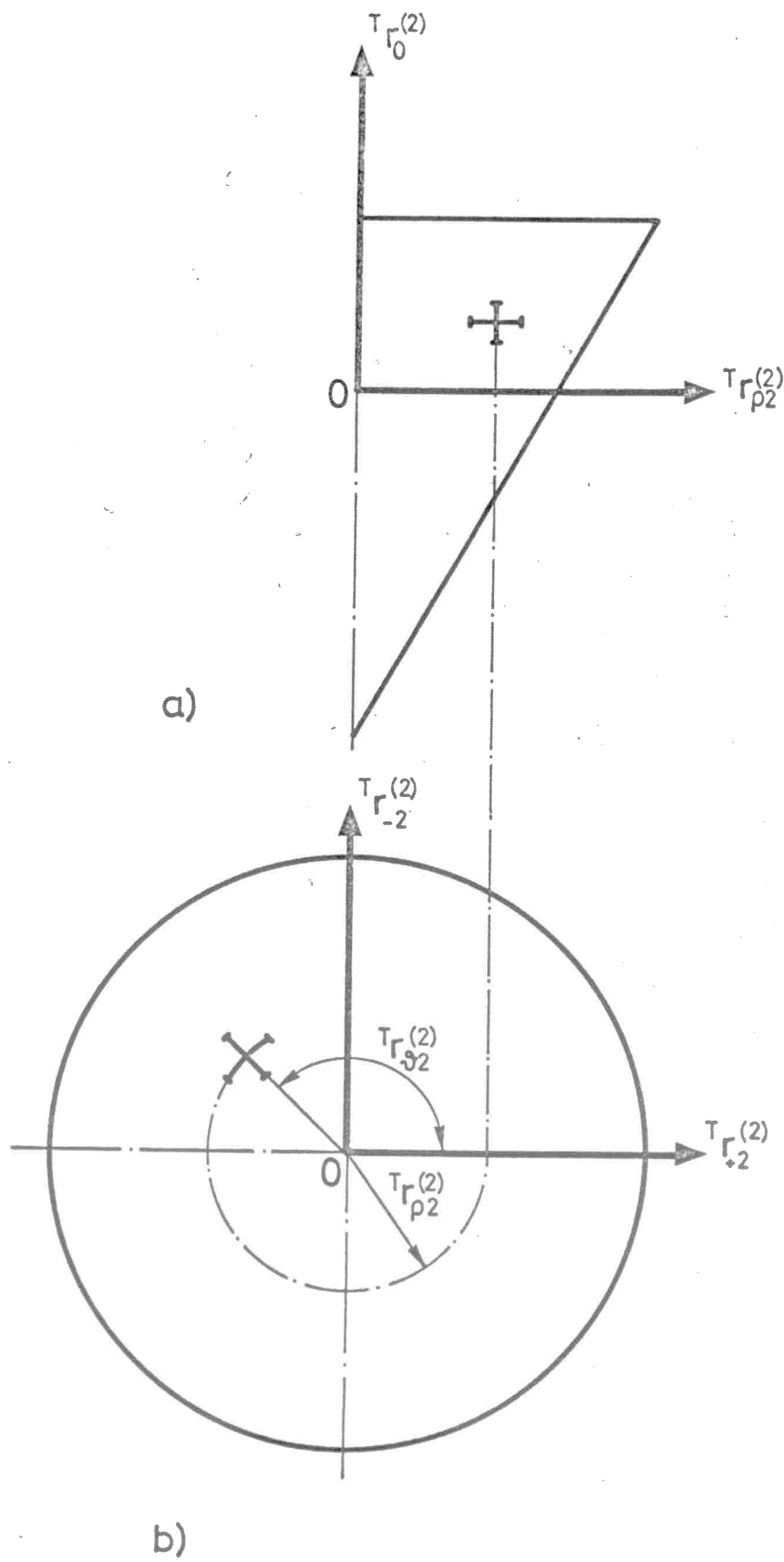
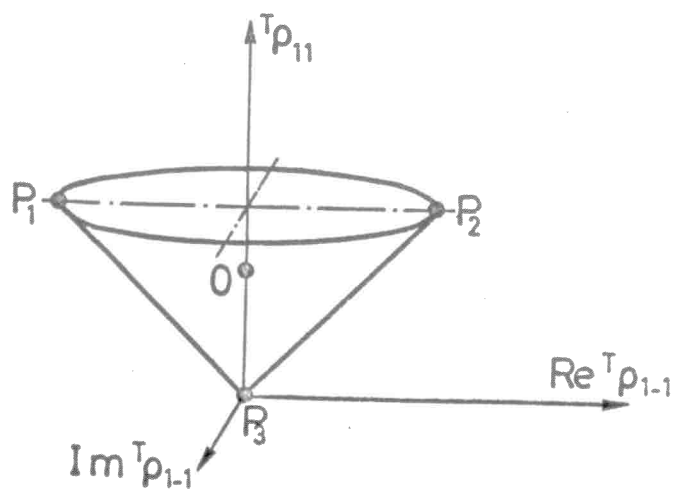
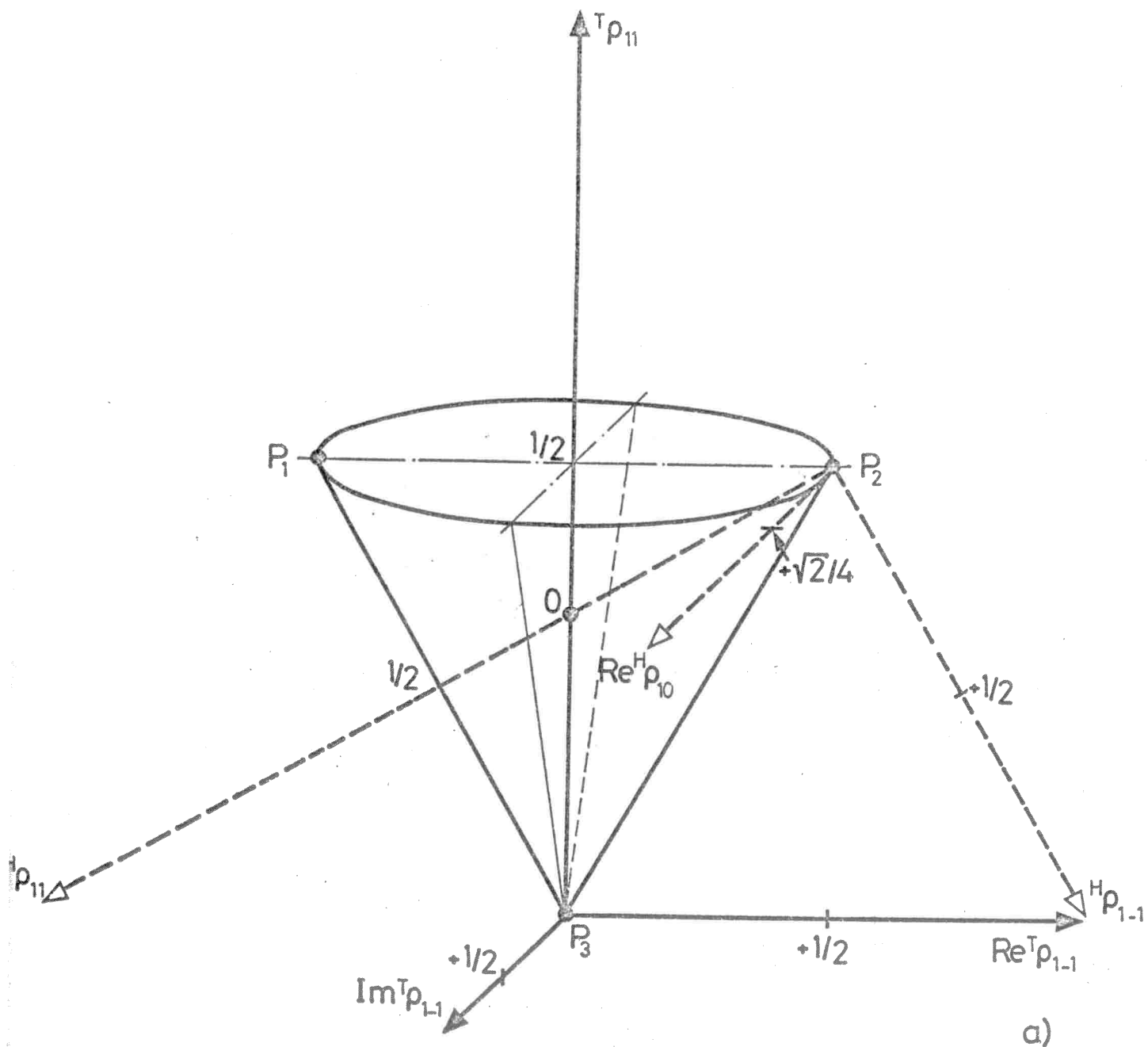
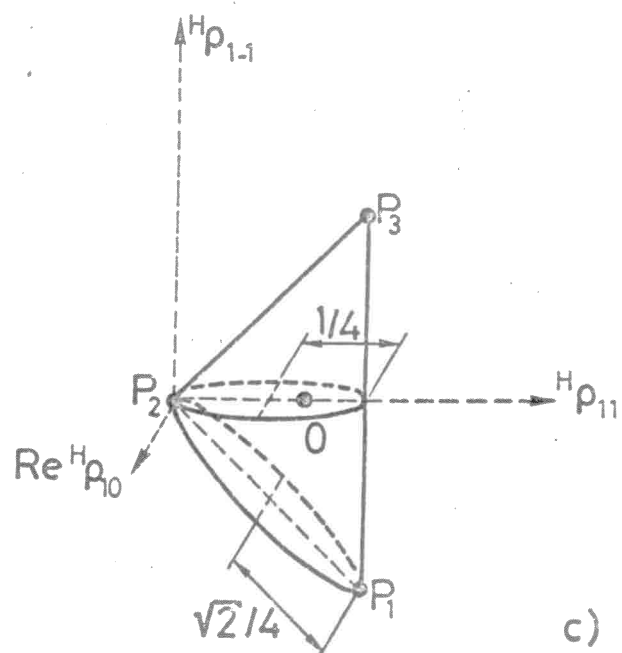


FIG. 2.2



b)



c)

FIG. 2.3

2. 4. Model predictions on the polarization of spin 1 particle

There are different models which predict relations between the three even B-symmetric polarization parameters of spin 1 particle, when it is produced in some particular type of reactions and/or reaction mechanisms. In our geometrical approach, such a model will simply fix inside the cone a certain subdomain, as locus of all representative points which are compatible with the predicted system of relations. In order to test experimentally these different models, it will be worthwhile showing inside the cone their predicted subdomains. The following points are an attempt to illustrate this geometrical approach for some particular models which are especially concerned with the two following types of reactions :

$$0^- \frac{1^+}{2} \longrightarrow 1^- \frac{1^+}{2} \quad (1)$$

$$0^- \frac{1^+}{2} \longrightarrow 1^- \frac{3^+}{2} \quad (2)$$

a. Predictions of t-channel exchange with fixed quantum numbers.

Some of these predictions on the polarization of the vector meson produced in reactions of type (1) and type (2), are visualized in Fig. 2. 4. In order to facilitate the comparison with the references which are going to be mentioned, the cone has been drawn with the three axes for the matrix elements ρ_{11} , ρ_{1-1} , $\text{Re } \rho_{10}$ in the t-helicity frame (Jackson system of parametrization). For the normalization of these axes see Fig. 2. 3. a) and c).

The OPE model, i. e., the exchange of spinless particles (necessarily 0^-) predicts as polarization subdomain the point P_2 (cf. Gottfried and Jackson, 64). The exchange of particles or trajectories of "normal parity" (i. e., $\sigma \equiv P (-1)^{J+1}$ or $J^P = 1^-, 2^+, 3^-, \dots$) predicts as polarization subdomain the segment P_3Q of the opposite generatrix. For exchange of "abnormal parity" (i. e., $\sigma = -1$, or $J^P = 1^+, 2^-, 3^+, \dots$) the prediction is a wedge of the cone, bounded by its circular base, P_1P_2 , and the elliptical section QP_2 , which is perpendicular to the generatrix P_1P_3 (cf. Ringland and Thews, 68; Thews, 69).

In the limit of Regge theories (i. e., for a small negative t , and very large s), these domains of normal and abnormal parity exchange shrink to the vertex of the cone P_3 , and to its base P_1P_2 (cf. Ader, Capdeville, Cohen-Tannoudji and Salin, 68). But in the actual high energy reactions, these subdomains will still

be some segment Q_3P_3 and a wedge of cone, bounded by its base and some section Q_1P_2 which is orthogonal to the plane $P_1P_2P_3$. The magnitude of these subdomains can be measured by the parameter

$$f = \frac{\overline{P_1Q_1}}{\overline{P_1Q}} = \frac{\overline{P_3Q_3}}{\overline{P_3Q}} \quad (3)$$

which is a well defined function of the four involved masses (m_1, m_2, m_3 and m_4 with the order corresponding to reactions (1) or (2)), and the variables s and t . Its terms of higher order in s are given by

$$f \cong \frac{2}{\text{ch}^2 \theta_t + 1} \quad (4a)$$

where

$$\text{ch} \theta_t = \frac{t^2 - t(2s - \sum_{i=1}^4 m_i^2) + (m_1^2 - m_3^2)(m_2^2 - m_4^2)}{\left[\Delta(t, m_1^2, m_3^2) \cdot \Delta(t, m_2^2, m_4^2) \right]^{1/2}} \quad (4b)$$

with

$$\Delta(x, y, z) = x^2 + y^2 + z^2 - 2xy - 2yz - 2zx \quad (4c)$$

In the "almost forward" region of high energy reactions the ratio f can be $1/10$ and less. In Fig. 2.5 and 2.6 the parameter f has been plotted versus t for several values of s and for the masses corresponding to the particular reactions $Kp \rightarrow K^*p$, and $Kp \rightarrow K^*N^*$. Remark that for maximal t , f is necessarily 1, and the prediction of the Regge limit cannot be applied. In fact, the colinearity condition of exact forward scattering imposes, as polarization subdomain, the segment P_2Q . Thus, the prediction of normal parity exchange at high energy is Q for completely forward direction and practically P_3 for a very small scattering angle. It would therefore be interesting if different polarization measurements for these neighbouring t intervals were done.

For reactions of type (1) without hypercharge exchange, the isoparity, G , of the exchange can be also considered. This consideration will be useful only in the case of abnormal parity exchange, and allow one to distinguish between the two planes of the predicted wedge (cf. Ringland and Thews, 68). By analogy with

$$\sigma = P(-1)^J \quad (5)$$

let us introduce the quantum number

$$\zeta = G(-1)^{I+J}, \quad (6)$$

where J and I stand for spin and isospin. The exchange of particles or trajectories of "abnormal parity" and "normal isoparity" (i. e., $\sigma = -1$ and $\zeta = +1$, or " π -type" of trajectory), predicts as polarization subdomain the base of the cone. For exchange of "abnormal parity" and "abnormal isoparity" (i. e., $\sigma = -1$ and $\zeta = -1$, or " A_1 - type" of trajectory), the prediction is the elliptical section Q_1P_2 , which is fixed by f , as function of s and t . Furthermore, when a single particle or trajectory is exchanged (hypothesis of real t -helicity amplitudes), these subdomains are reduced to their circular or elliptical boundaries.

A simple peripheral model, with the higher symmetry $SU(6)$ for each vertex, predicts a well defined mixture of pseudoscalar and vector exchanges, i. e., a point inside the triangle P_2P_3Q . For each reaction of type (1) or type (2), this point is fixed as a parameter free function of the involved masses and the variables s and t (cf. Doncel, 67).

b) Predictions of the quark model.

For reactions of type (2), the quark model predicts some relations between the three even B -symmetric polarization parameters of particle 1^- and the three ones of particle $\frac{3}{2}^+$. They will be considered in 4. 4.

c) Predictions of s-helicity conservation.

The hypothesis of s -helicity conservation has been proposed recently for several two-body reactions in which spin 1 particle is produced from initial pseudoscalar or initial photon. (cf. Gilman, Pumplin, Schwimmer, and Stodolsky, 70). In the former case the predicted subdomain is the point P_2 in Fig. 2. 4., but interpreted now as corresponding to a s -frame of quantization. Remark that the rotation angle around the normal which transforms a t -frame into an s (or u) frame may be considerable also for small scattering angle (cf. I. A. 1). The points predicted by s (or u) helicity conservation and those predicted by t -helicity conservation are separated by a double rotation angle around the axis of the cone, and therefore can be clearly distinguished. For this kind of experimental test it is specially recommended that the angular polarization parameter of Fig. 2. 2. b) be measured and drawn for the three different frames.

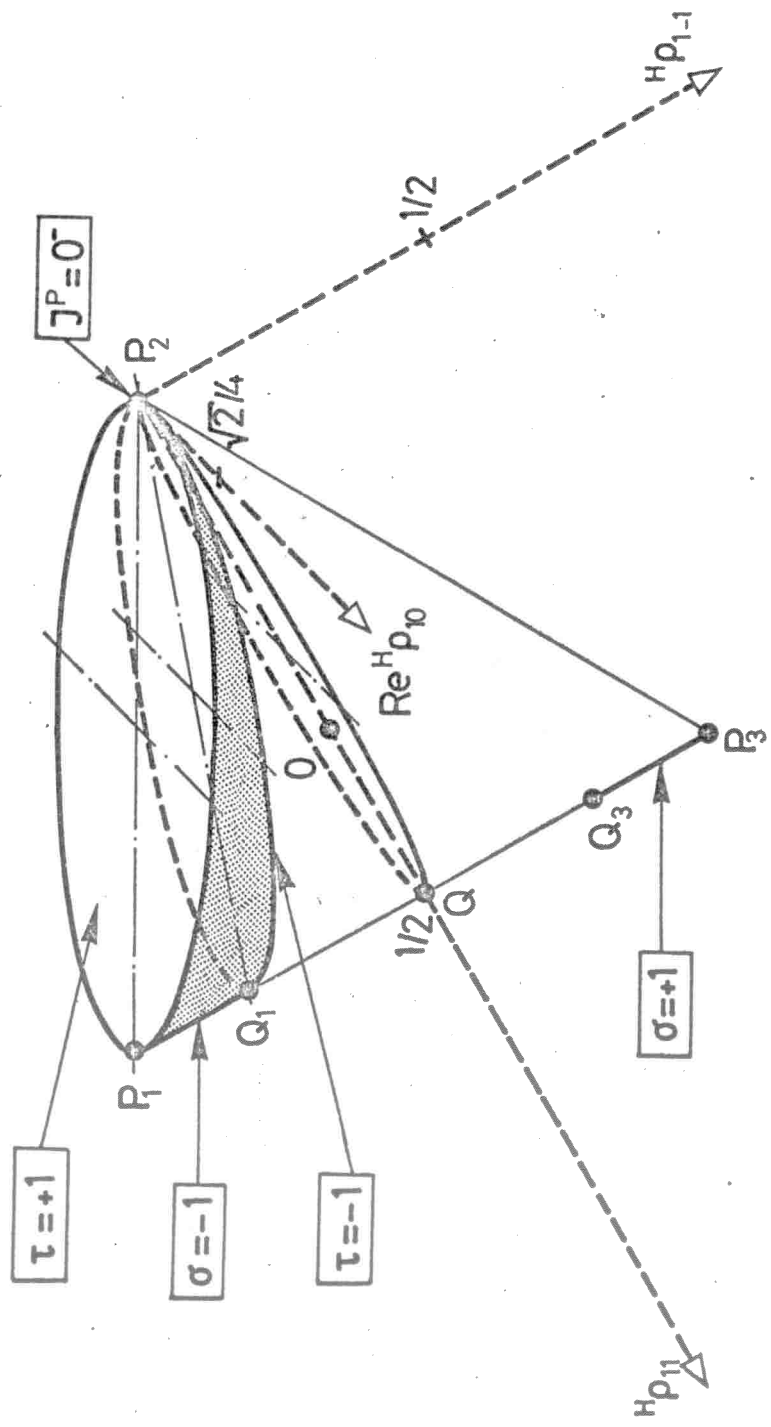


FIG. 2.4 - Polarization subdomains predicted by t-channel exchange with fixed quantum numbers : $\sigma = P(-1)^J$, $\tau = G(-1)^{J+1}$. The shrinking of these subdomains in the Regge-limit can be estimated by the parameter

$$f = \frac{P_1 Q_1}{P_1 Q} = \frac{P_3 Q_3}{P_3 Q}$$

FIG.2.4

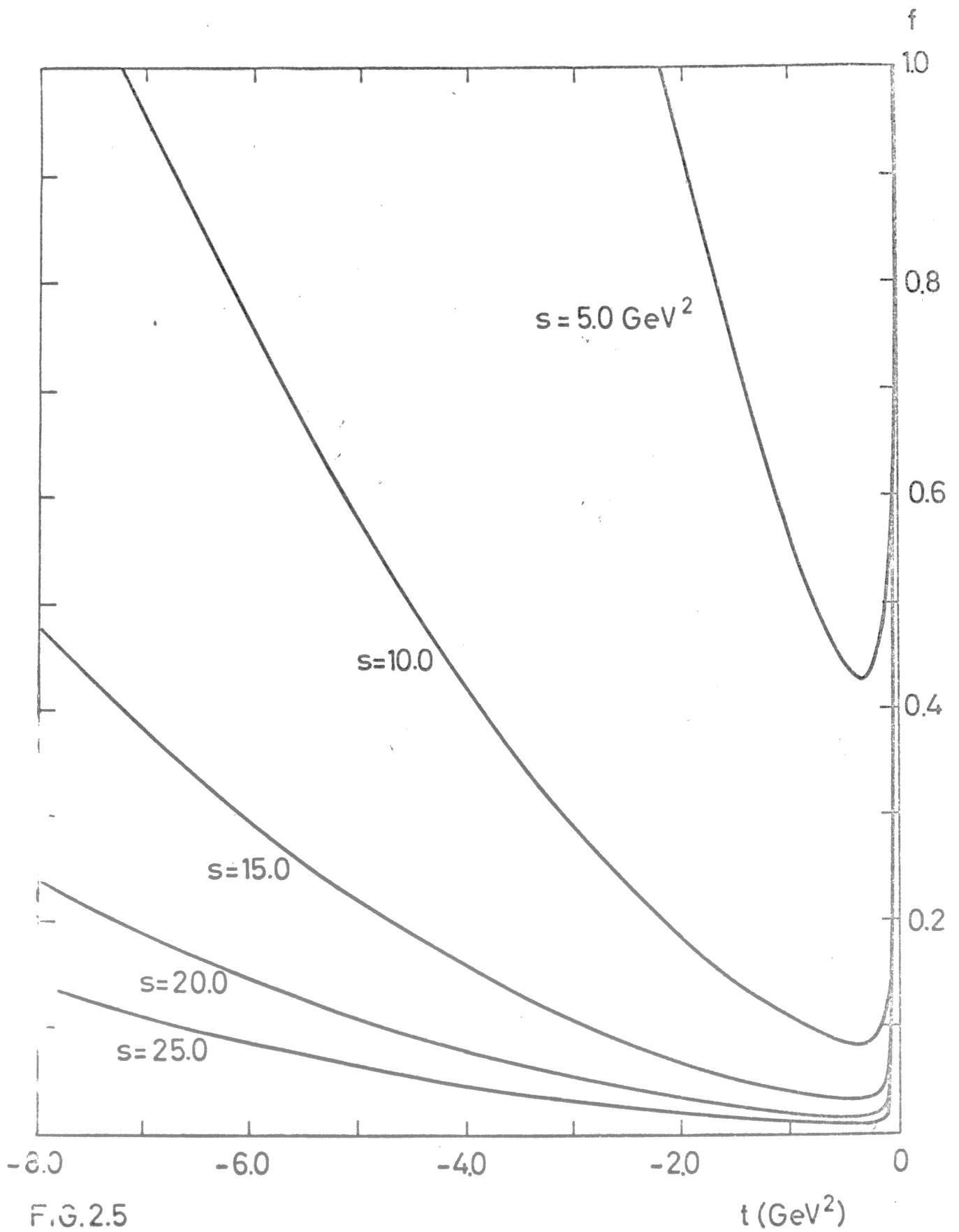


FIG. 2.5 - Values of the Regge-limit parameter f , as function of s and t , for the type (1) reaction : $KP \rightarrow K^*P$.

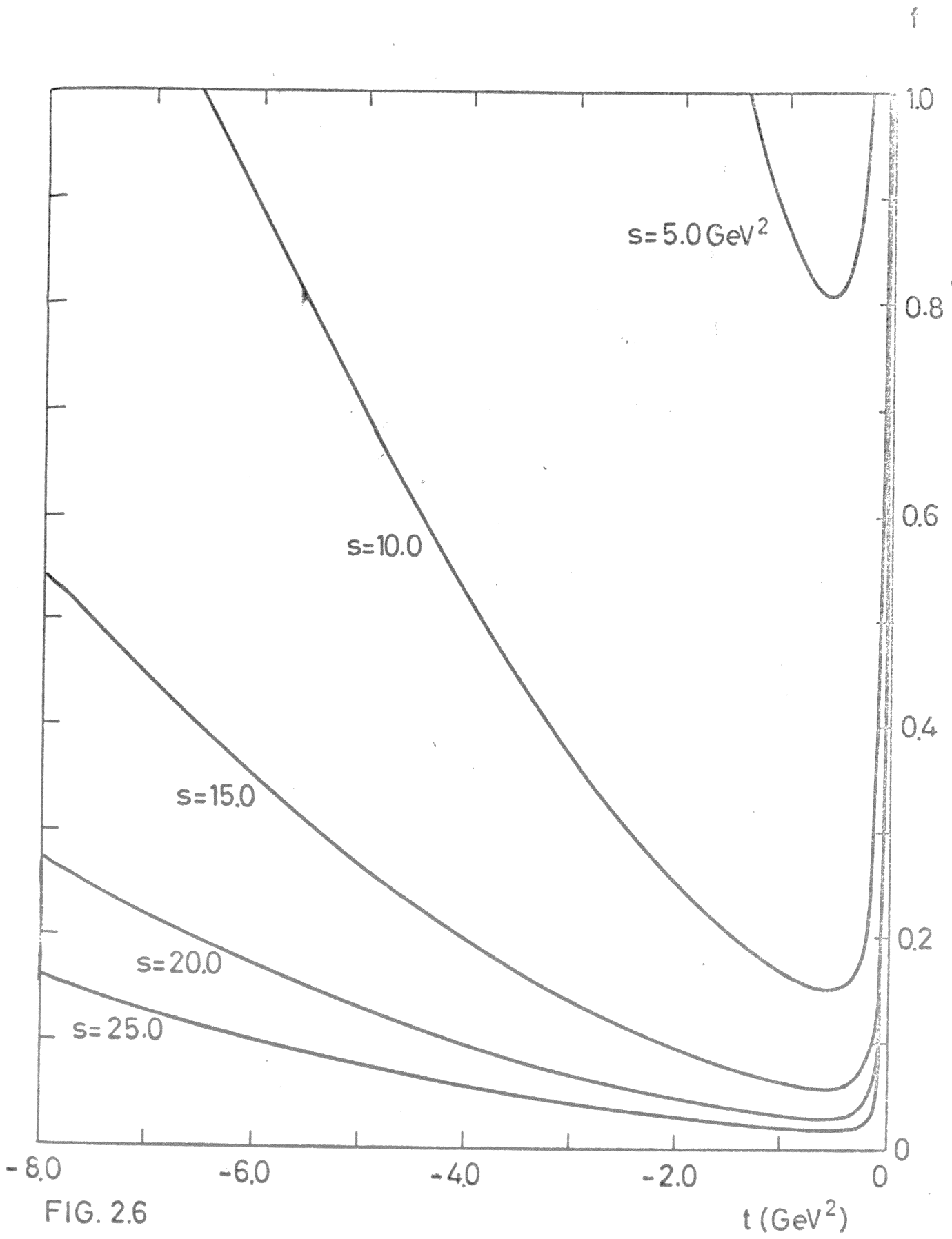


FIG. 2.6 - Values of the Regge-limit parameter f , as function of s and t , for the type (2) reaction $K P \rightarrow K^* N^*$.

2. Even polarization of spin 3/2 particles.3. 1. Measurement of the even polarization of spin 3/2 particle.

The most common decay of spin 3/2 particle is the strong two-body decay into one spinless particle and one spin 1/2 particle, as indicated in Table 3.1 (a). Angular momentum and parity conservations allow one decay amplitude. The angular distribution depends only on the even polarization parameters $t_M^{(2)}$ or $r_M^{(2)}$, and has the form given in Table 3.1 (b) or (c) (cf. I. A. 4). The inverse expressions, which supply a method of independent measurement for each multipole parameter, are given also in Table 3.1 (d) and (e). The angular brackets $\langle \dots \rangle$ indicate experimental mean values of the enclosed expressions for the ensemble of events. $Y_M^{(2)}$ are the usual spherical harmonics. Their arguments θ, φ are the polar and azimuthal angles, fixing for each event the direction of any of the decay products, in any frame in which the spin 1 particle is at rest.

In the case of B-symmetry for the production process of the spin 3/2 particle (i. e., production in a parity conserving reaction with unpolarized target and beam, cf. I. A. 3.), two of these five even polarization parameters have to be zero (see Table 0.1. (c)). For transversity quantization (quantization along the normal of the production plane) the two multipole parameters $r_M^{(2)}$ with M odd have to be zero, whilst for helicity quantization (quantization along any direction inside the production plane) the two multipole parameters $r_M^{(2)}$ with M negative must be zero, as indicated in Table 3.1 (f) and (g).

The odd polarization parameters of spin 3/2 particle $r_M^{(1)}$, $r_M^{(3)}$ or $t_M^{(1)}$, $t_M^{(3)}$, cannot be measured from the angular distribution of the two body decay. But they can be measured whenever the polarization of the spin 1/2 decay product is observed. For instance in the case of cascade decay (cf. 4.1).

TABLE 3.1. - Measurement of the even polarization of spin $\frac{3}{2}$ particle

Decay	
(a)	$\frac{3}{2} \rightarrow \frac{1}{2} + 0$ (strong interaction)
Angular distribution	
(b)	$I(\theta, \varphi) = \frac{1}{4\pi} - \sqrt{\frac{1}{4\pi}} \sum_{M=-2}^{+2} \bar{t}_M^{(2)} Y_M^{(2)}(\theta, \varphi)$
(c)	$I(\theta, \varphi) = \frac{1}{4\pi} [1 - \sqrt{\frac{3}{4}} r_0^{(2)} (3 \cos^2 \theta - 1) - \frac{3}{2} \sin^2 \theta (r_2^{(2)} \cos 2\varphi + r_{-2}^{(2)} \sin 2\varphi) - \frac{3}{2} \sin 2\theta (r_1^{(2)} \cos \varphi + r_{-1}^{(2)} \sin \varphi)]$
Multipole parameters	
(d)	$t_M^{(2)} = -\sqrt{4\pi} \langle Y_M^{(2)}(\theta, \varphi) \rangle \quad M = -2, -1, \dots, +2$
(e)	$r_0^{(2)} = \sqrt{\frac{5}{3}} t_0^{(2)}$
	$r_M^{(2)} = (-1)^M \sqrt{\frac{10}{3}} \operatorname{Re} t_M^{(2)} \quad M = 1, 2$
	$r_{-M}^{(2)} = (-1)^M \sqrt{\frac{10}{3}} \operatorname{Im} t_M^{(2)}$
Condition of B-symmetry in the production process	
(f)	For transversity quantization
	$T_{r_1}^{(2)} = T_{r_{-1}}^{(2)} = 0$
(g)	For helicity quantization
	$H_{r_{-2}}^{(2)} = H_{r_{-1}}^{(2)} = 0$

3.2. Relation between different even polarization parameters of spin 3/2 particles

For anyone reference frame, the even part of the density matrix of spin 3/2 particle has the form indicated in Table 3.2 (a) (cf. I. A. 6.). The very elements of this even density matrix can be used as polarization parameters. They are related to the measurable multipole parameters of Table 2.1 by the relations given in Table 3.2 (b).

For each particle, several pairs of reference frames for transversity and helicity quantization can be intrinsically defined. Each pair of frames is fixed by the normal to the production three-plane and some space or time-like direction (like the four-momentum transfer, which is associated with the s, t, or u channel of a two-body reaction, cf. I. A. 1.). Associated transversity and helicity frames are simply related in the standard conventions by a rotation of $\frac{\pi}{2}$ radians around the x-axis. The corresponding linear transformation on the multipole parameters are given in Table 3.2 (c), where the left T and H superscripts refer to transversity and helicity quantizations.

Two different pairs of transversity-helicity frames, say a and b, are related through a rotation around the normal by an angle Ψ_{ba} (which usually will be a complicated function of the kinematical invariants s, t, u of a two-body reaction, cf. I. A. 1.). The corresponding linear transformation on the multipole parameters is very simple for the transversity quantization. It is also given in Table 3.2 (d), where the left subscripts a, b, label any transversity frame.

As has been mentioned, in the case of B-symmetric production the transversity multipole parameters with M odd or the helicity multipole parameters with M negative must be zero. They are the parameters written in the second column of Table 5.2 (c), and in the last line or column of Table 3.2(b). Note that in this case for transversity quantization the matrix element ρ_{31} is zero, and the density matrix in Table 3.2 (a) has a "checker-board pattern", while for helicity quantization the imaginary parts of ρ_{31} and ρ_{3-1} are zero, and the density matrix is real.

TABLE 3.2. - Relation between different even polarization parameters of spin $\frac{3}{2}$ particle

<p>(a) Even part of the density matrix for spin $\frac{3}{2}$ particle</p> $\rho^e = \begin{vmatrix} \rho_{33}^e & \rho_{31}^e & \rho_{3-1}^e & 0 \\ \rho_{31}^e & \rho_{11}^e & 0 & \rho_{3-1}^e \\ \rho_{3-1}^e & 0 & \rho_{11}^e & -\rho_{31}^e \\ 0 & \rho_{3-1}^e & -\rho_{31}^e & \rho_{33}^e \end{vmatrix} \quad \rho_{11}^e = \frac{1}{2} - \rho_{33}^e$	
<p>(b) Relation between the matrix elements in (a) and the multipole parameters in Table 3.1 .</p> $\begin{array}{l l} r_0^{(2)} = \sqrt{\frac{4}{3}} (\rho_{33}^e - \rho_{11}^e) & \text{(BH)} \\ r_2^{(2)} = \sqrt{\frac{16}{3}} \operatorname{Re} \rho_{3-1}^e & r_{-2}^{(2)} = -\sqrt{\frac{16}{3}} \operatorname{Im} \rho_{3-1}^e \\ \hline \text{(BT)} \quad r_1^{(2)} = \sqrt{\frac{16}{3}} \operatorname{Re} \rho_{31}^e & r_{-1}^{(2)} = -\sqrt{\frac{16}{3}} \operatorname{Im} \rho_{31}^e \end{array}$	
<p>(c) Relation between the multipole parameters for transversity and helicity quantizations</p> $\begin{array}{l l} H_{r_0}^{(2)} = -\sqrt{\frac{1}{4}} T_{r_0}^{(2)} - \sqrt{\frac{3}{4}} T_{r_2}^{(2)} & \text{(B)} \\ H_{r_2}^{(2)} = -\sqrt{\frac{3}{4}} T_{r_0}^{(2)} + \sqrt{\frac{1}{4}} T_{r_2}^{(2)} & H_{r_{-2}}^{(2)} = T_{r_1}^{(2)} \\ H_{r_1}^{(2)} = -T_{r_{-2}}^{(2)} & H_{r_{-1}}^{(2)} = -T_{r_{-1}}^{(2)} \end{array}$	
<p>(d) Relation between the multipole parameters for two different transversity quantizations (rotation on the normal of angle ϕ_{ba})</p> $\begin{array}{l} T_{b^r_0}^{(2)} = T_{a^r_0}^{(2)} \\ T_{b^r_M}^{(2)} = \cos(M\phi_{ba}) T_{a^r_M}^{(2)} - \sin(M\phi_{ba}) T_{a^r_{-M}}^{(2)} \\ T_{b^r_{-M}}^{(2)} = \sin(M\phi_{ba}) T_{a^r_M}^{(2)} + \cos(M\phi_{ba}) T_{a^r_{-M}}^{(2)} \end{array} \quad \begin{array}{l} \\ M = 1, 2 \\ \text{(B2)} \end{array}$	

(BH) For B-symmetry and helicity quantization, the parameters in this column are zero.

(BT) For B-symmetry and transversity quantization, the parameters in this line are zero.

(B) For B-symmetry, the parameters in this column are zero.

(B2) For B-symmetry, $M = 2$.

3.3. Polarization domain for B-symmetric spin 3/2 particle.

The domain of possible values of the three even polarization parameters of a B-symmetric spin 3/2 particle is fixed by the requirement that the full density matrix including eventually same odd part, must be positive, i. e., the probabilities of the different pure states present in the statistical mixture, must be positive (cf. I. A. 6.).

This "polarization domain" can be studied intrinsically, i. e., independently of any concrete basis for the polarization parameters. With the conveniently normalized intrinsic metric of the matrix space, it is a sphere of radius $\sqrt{\frac{1}{3}}$ (see Fig. 3.1). The unpolarized state is represented by its center, O. The distance of any representative point to this "isotropy center" gives directly the degree of even polarization of the corresponding state. This shows that pure states of only even polarization cannot exist. But, as it will be shown in 4.4, to each representative point on the spherical surface corresponds a couple of B-symmetric orthogonal pure states. They are not even, but their fifty-fifty mixture is the even state represented by the point. The two couples of pure states corresponding to diametrically opposite points of the spherical surface, are orthogonal to each other. Any intermediate point of the diameter will represent a mixture of these two pairs of pure states, with the same probability for both states in each pair. If these two probabilities are materialized by weights at the corresponding extremes of the diameter, the representative point is situated at their barycenter. This description as mixture of four orthogonal B-symmetric pure states, is unique for any point inside the sphere except the isotropy center.

A concrete frame of quantization will allow to fix a basis for the polarization parameters, and to write down the inequalities defining this polarization domain. Table 3.3. gives the inequalities, and Fig. 3.1 indicates the axes of the normalized multipole parameters, $r_M^{(2)}$, for any pair of associated transversity and helicity frames of quantization. As shown by the relations of Table 3.2 (c), they are related through a rotation of π radians around the axis a

If the quantization frames are rotated by an angle ψ_{ba} around the normal, according to Table 3.2 (d), the parameter axes of Fig. 3.1. are in turn rotated by an angle $2 \cdot \psi_{ba}$ around the axis $r_O^{(2)}$ of the sphere.

For transversity quantization, and labelling pure states by the magnetic quantum number, the point P_1 represents an equiprobable mixture of the pair of pure states $|+3/2\rangle$ and $|-3/2\rangle$. The point P_2 represents an analogous mixture of the pair $|+1/2\rangle$ and $|-1/2\rangle$. A general point on the spherical surface with polar and azimuthal angles Θ and Φ (we take $T_{r_0}^{(2)}$ as * origin of azimuths, and $T_{r_2}^{(2)}$ $T_{r_{-2}}^{(2)}$ as their positive sens) represents an equiprobable mixture of the pair of B-symmetric pure states

$$|\Theta, \Phi, \pm\rangle = \cos \frac{\Theta}{2} |\pm 3/2\rangle + \sin \frac{\Theta}{2} e^{\pm i\Phi} |\pm 1/2\rangle \quad (I)$$

It is easy to check the orthogonality of these pairs of pure states with the pair corresponding to the diametrically opposite point :

$$|\pi - \Theta, \Phi + \pi, \pm\rangle = \sin \frac{\Theta}{2} |\pm 3/2\rangle - \cos \frac{\Theta}{2} e^{\pm i\Phi} |\pm 1/2\rangle \quad (II)$$

The general point inside the sphere with spherical coordinates Θ, Φ and ρ will be the mixture of these four pure states with probabilities $\frac{1 + \sqrt{3}\rho}{4}$ for each state (I) and $\frac{1 - \sqrt{3}\rho}{4}$ for each state (II).

For helicity quantization the equiprobable mixture of the pure states $|+3/2\rangle$ and $|+1/2\rangle$ will be represented by the points Q_1 and Q_2 . And by rotation of the frame around the normal Q_1 and Q_2 generate two "parallels" of latitude $\pm 30^\circ$ corresponding to this kind of mixtures, for quantization along different directions inside the production plane. (For other axis of quantization outside the production plane and the normal, this kind of mixture is not B-symmetric).

Therefore any such rotations around the normal leave invariant the polarization parameters $T_{r_0}^{(2)}$ and $T_{r_2}^{(2)} \equiv \sqrt{[T_{r_2}^{(2)}]^2 + [T_{r_{-2}}^{(2)}]^2}$. Thus a convenient two-dimensional representation of the points inside the sphere, that displays their cylindrical coordinates, is proposed in Fig. 3.2. Its diagram a) presents these two polarization parameters which are invariant under rotations of the quantization axis around the normal. In this diagram, the representative points must be the same for measurements corresponding to s, t or u frames of quantization. The degrees of even polarization are intuitively seen as the distances of the points to the origin 0. The positivity conditions require that the points be inside the half circle. Their distance to the origin 0 shows directly the degree of even polarization. The coordinates Θ and ρ which allow the

* Erratum : ... as polar axis, $T_{r_2}^{(2)}$ as ...

interpretation of the mixture are there evident. On the other hand, diagram b) of Fig. 2.2 giving the angle $\phi = \arctan \frac{r_M^{(2)}}{r_2^{(2)}}$ of these coordinates, depends completely on the chosen transversity parametrization. Because of this it would be worthwhile to measure and to draw this diagram for s, t and u frames of quantization.

Instead of the normalized multipole parameters, $r_M^{(2)}$, one could use the density matrix elements, let us say ρ_{33}^e , $\text{Re } \rho_{3-1}^e$ and $\text{Im } \rho_{3-1}^e$ for transversity, and ρ_{33}^e , $\text{Re } \rho_{3-1}^e$ and $\text{Re } \rho_{31}^e$ for helicity quantization (so, e.g., Gottfried and Jackson, 64, for t-helicity quantization).

According to Table 3.2 (a) and (b), the transversity and helicity axes represented in Fig. 3.1 will be translated to the points P_2 and Q_2 respectively, and one scale factor has to be introduced. That has been shown in Fig. 3.3.

Notice that in Figs. 3.1 to 3.3, only the three even parameters of a B-symmetric density matrix are represented. The complete domain of even and odd polarization is discussed in 4.3.

TABLE 3.3. - Positivity conditions for the even polarization parameters of B-symmetric spin $\frac{3}{2}$ particle

(a) Positivity conditions for transversity parametrization

$$[T_{r_2}^{(2)}]^2 + [T_{r_{-2}}^{(2)}]^2 + [T_{r_0}^{(2)}]^2 \leq \sqrt{\frac{1}{3}}$$

(b) Positivity conditions for helicity parametrization

$$[H_{r_0}^{(2)}]^2 + [H_{r_1}^{(2)}]^2 + [H_{r_2}^{(2)}]^2 \leq \sqrt{\frac{1}{3}}$$

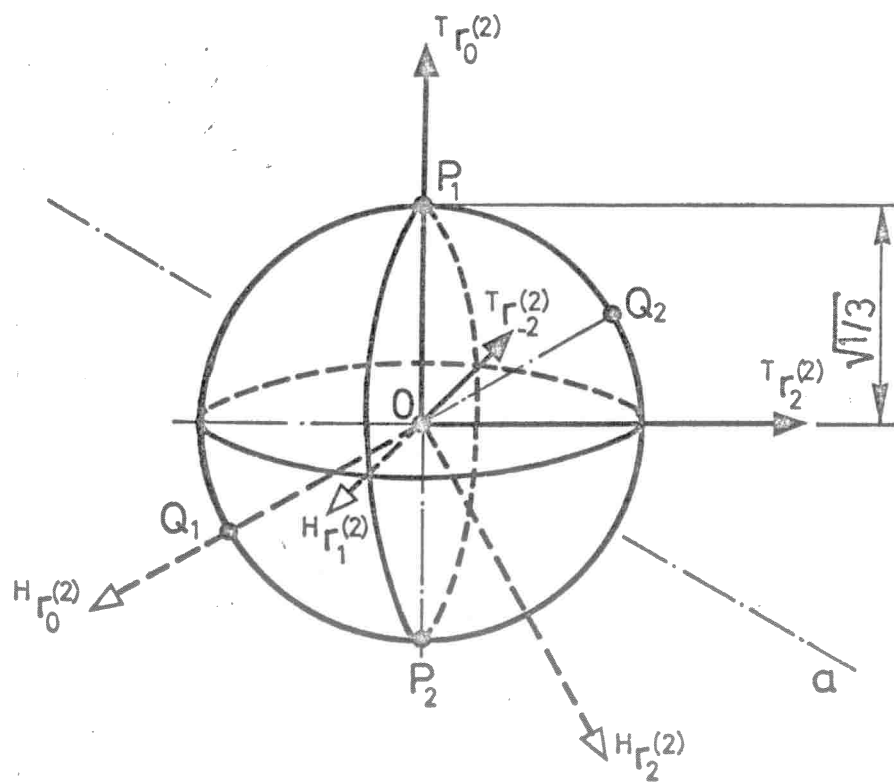


FIG. 3.1

FIG. 3.1 - Domain of the even, B-symmetric polarization of spin 3/2 particle.

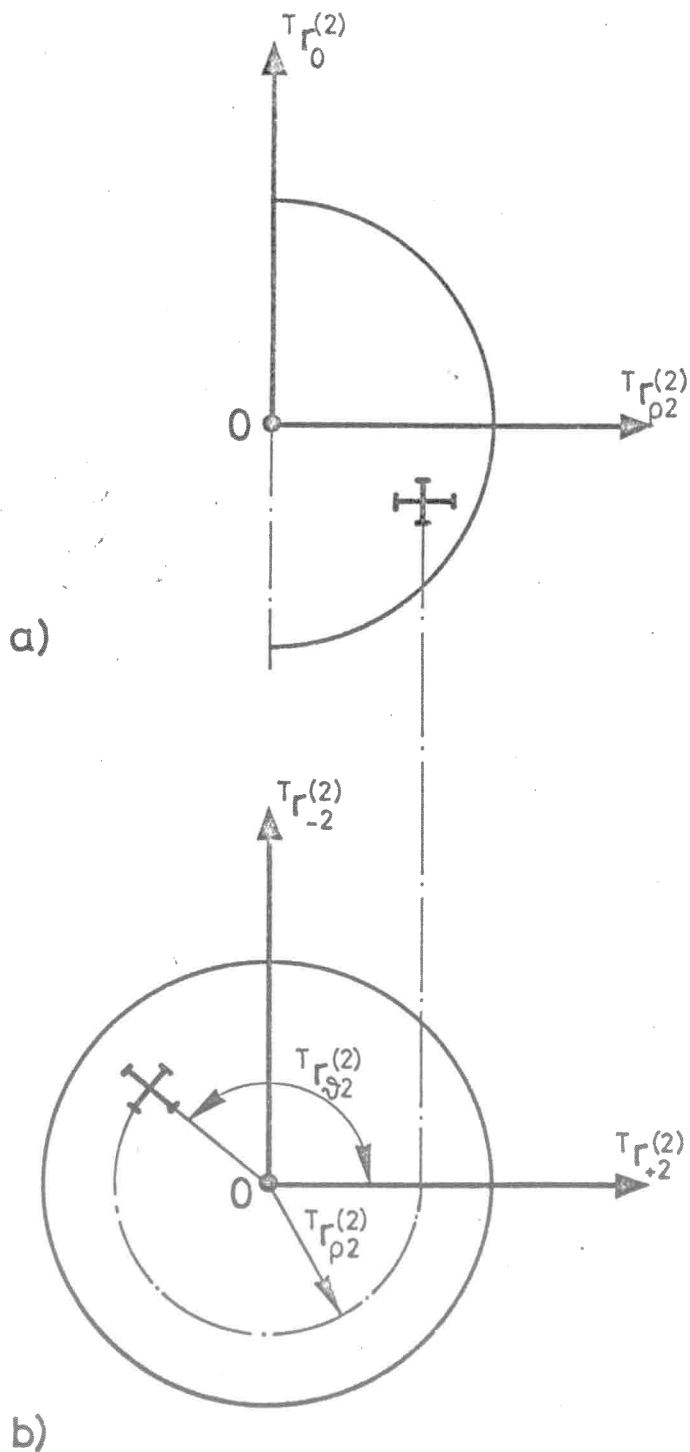
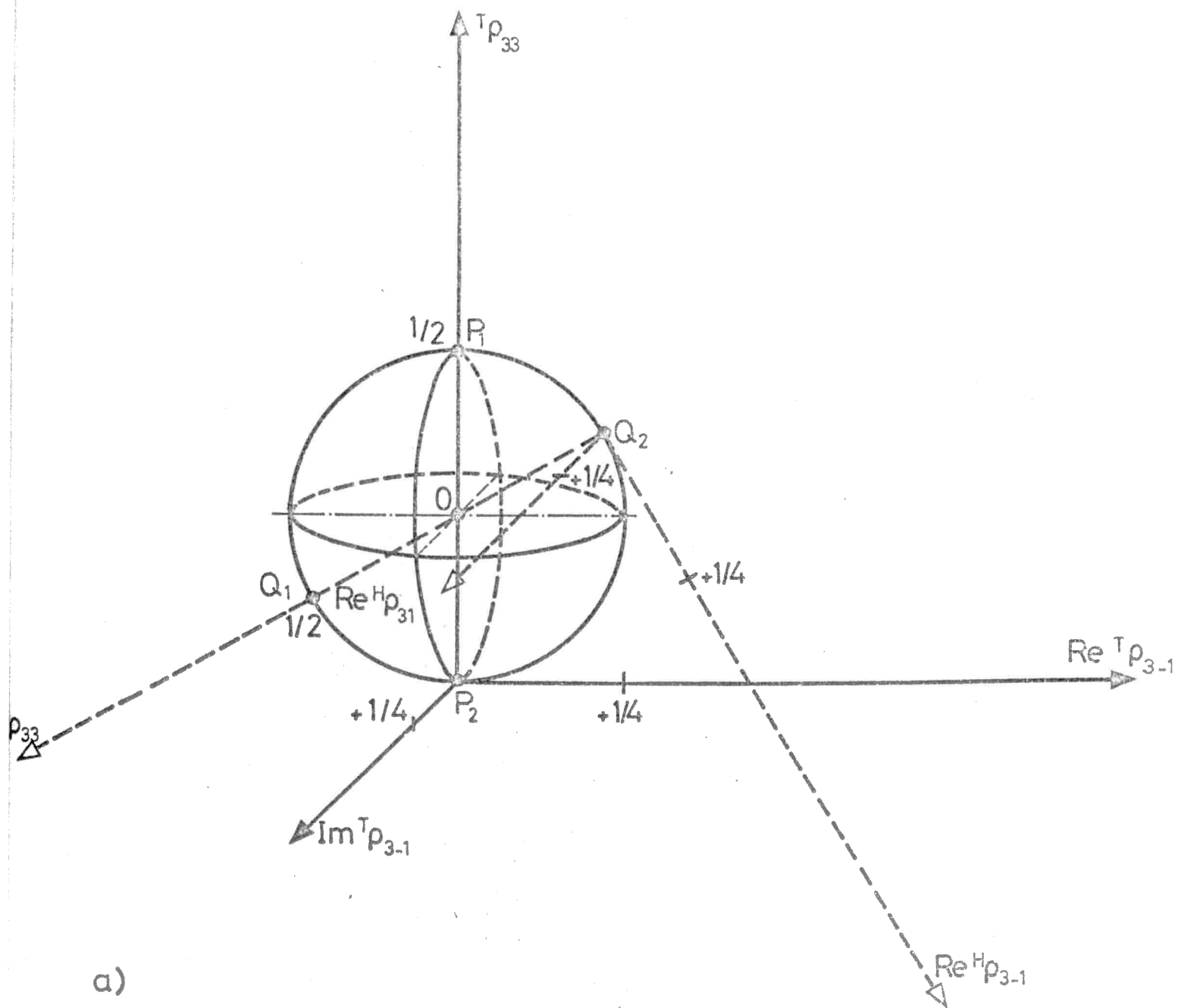
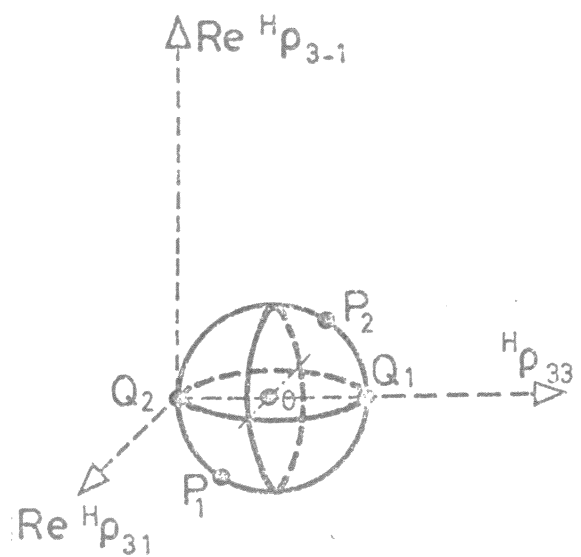
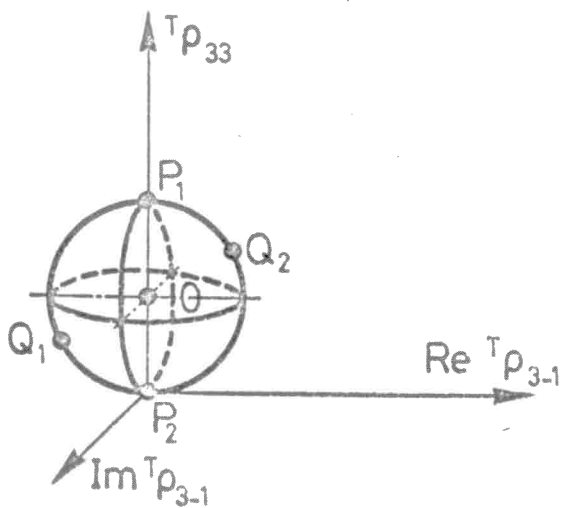


FIG. 3.2

FIG. 3.2 - Two-dimensional diagrams for plotting experimental points inside the polarization domain in FIG. 3.1 : a) Meridian section. The plotted point is invariant under frame rotations around the normal. b) Vertical projection. The azimuth of the plotted point is different for s, t, and u frames of quantization.



a)



3.4 Model predictions on the even polarization of spin 3/2 particle.

There are different models which predict relations between the three even B-symmetric polarization parameters of spin 3/2 particle, when it is produced in some particular type of reactions and / or reaction mechanisms. In our geometrical approach, such a model will simply fix inside the sphere of polarization a certain subdomain, as locus of all representative points which are compatible with the predicted system of relations. In order to test experimentally these different models, it will be worthwhile showing inside the sphere their predicted subdomains. The following points are an attempt to illustrate this geometrical approach for some particular models which are especially concerned with the following types of reactions :

$$0^- \quad \frac{1}{2}^+ \quad \longrightarrow \quad 0^- \quad \frac{3}{2}^+ \quad (1)$$

$$0^- \quad \frac{1}{2}^+ \quad \longrightarrow \quad 1^- \quad \frac{3}{2}^+ \quad (2)$$

$$\frac{1}{2}^+ \quad \frac{1}{2}^+ \quad \longrightarrow \quad \frac{1}{2}^+ \quad \frac{3}{2}^+ \quad (3)$$

a. Prediction of the Stodolsky-Sakurai model.

For reaction of type (1), in which the pseudoscalar exchange is forbidden, the hypothesis of vector meson exchange with only magnetic dipole coupling in the baryonic vertex has been made, by analogy to the photon coupling in isobar photoproduction (cf. Stodolsky and Sakurai, 63 ; Stodolsky, 64). The predicted polarization subdomain for the spin 3/2 particle is the point P_2 in Figs. 3.1 or 3.3.

b. Predictions of t-channel exchange with fixed quantum numbers.

For reactions of type (1) there are no predictions from the quantum numbers of the t-exchange. But the rank 2 condition of the density matrix predicts a relation between the odd and even polarizations of spin 3/2 particle, which will be studied in 4.4. And the hypothesis of single particle or trajectory exchange (i. e., real t-helicity amplitudes) predicts as subdomain for the even polarization the whole surface of the sphere (cf. Ringland and Thews, 68).

For reactions of type (2) and in the limit of Regge theories, the exchange of single particle or trajectory with normal parity predicts also the

surface of the sphere. But in the actual high energy reactions this predicted subdomain will be a certain thick shell of the sphere. The maximal thickness of this shell related to the radius of the sphere has as upper limit the same parameter f defined in eqs. 2.4. A better upper limit for the variable thickness of this shell has been evaluated (cf. Thews, 69), and is shown in Fig. 3.4. The predicted subdomain is bounded by the sphere and an ellipsoid which is tangent to the sphere in Q_1 and Q_2 . The length of the other semi-axes related to the radius of the sphere are

$$\frac{\overline{R'_1 O}}{R_1 O} = \frac{\overline{R'_2 O}}{R_2 O} = 1 - f \quad (4)$$

$$\frac{\overline{S'_1 O}}{S_1 O} = \frac{\overline{S'_2 O}}{S_2 O} = \sqrt{1-f} = 1 - \frac{1}{2}f - \frac{1}{8}f^2 - \dots$$

Recall that for completely forward scattering f is 1, and no prediction can be done. In fact, the colinearity condition imposes the diameter $Q_1 Q_2$ as polarization subdomain.

Remark that this prediction for reactions of type (2) can be applied only when the polarization measurement of the spin 1 particle allows the hypothesis of normal parity exchange, i. e., when the representative point lies in the segment $P_3 Q_3$ of Fig. 2.3. On the contrary, when it lies in P_2 (as abnormal parity exchange allows, and 0^- exchange imposes), the same hypothesis of single particle or trajectory exchange predicts, as polarization subdomain for the spin 3/2 particle, the very surface of the sphere (and its point Q_2 in the case of 0^- exchange).

Simple peripherism with the higher symmetry $SU(6)_w$ for each vertex is equivalent to the Stodolsky - Sakurai model for reactions of type (1) (cf. Harari and Lipkin, 65). But for reactions of type (2) such a model fixes a certain mixing of pseudoscalar exchange and vector exchange with magnetic dipole coupling. (Doncel, 67). Thus it predicts for the spin 3/2 particle a well defined polarization point inside the semi-circle $Q_2 P_2 Q_1$, which is identical to the point p predicted for the spin 1 particle produced in the same reaction and at the same values of s and t . I. e., if the cone (reduced by a factor $\sqrt{3}$) is inscribed in the sphere, with the same orientation for the axes of the t -frame multipole parameters, both points must coincide.

c. Predictions of the quark model.

For reactions of type (1), the prediction of the quark model is also the same as the prediction of the Stodolsky-Sakurai model.

For reactions of type (2), the quark model predicts some relations between the polarization of spin 1 and that of spin 3/2 particle. There are three kinds of predictions (cf. Bialas and Zalewski, 68). The first and more clear-cut kind of predictions relates the heights of the representative points inside the cone and the sphere, or inside their meridian sections which have been represented in diagram a) of Figs. 2. 3. and 3. 3. I. e., if the half equilateral triangle (reduced by a factor $\sqrt{3}$) is inscribed in the semi-circle, both representative points must lie at the same level. The second kind of predictions relates completely the polarization of both particles, but in a non well defined frame of quantization, which could correspond to the t-frame, or perhaps to the s-frame. This would mean that for the mentioned superposition of diagrams a) both points must coincide, and that the angular polarization parameters represented in the diagram b) of the same Figs. 2. 3 and 3. 3. must have the same value for a t-frame or perhaps for a s-frame of quantization. The third kind of predictions says that this value must be zero.

This last kind of prediction is also valid for the spin 3/2 particle produced in reaction of type (3).

d. Predictions of s-helicity conservation.

The hypothesis of s-helicity conservation has been proposed recently also for reactions of type (1) and type (3) (cf. Gilman, Pumplin, Schwimmer, and Stodolsky, 70). This hypothesis predicts as polarization subdomain for the spin 3/2 particle the point Q_2 in Figs. 3. 3. or 3. 4., but interpreted now as corresponding to a s-frame of quantization. Also for this experimental test it is specially recommended that the angular polarization parameter of diagram b) in Fig. 3. 2. be measured and drawn for the three different frames.

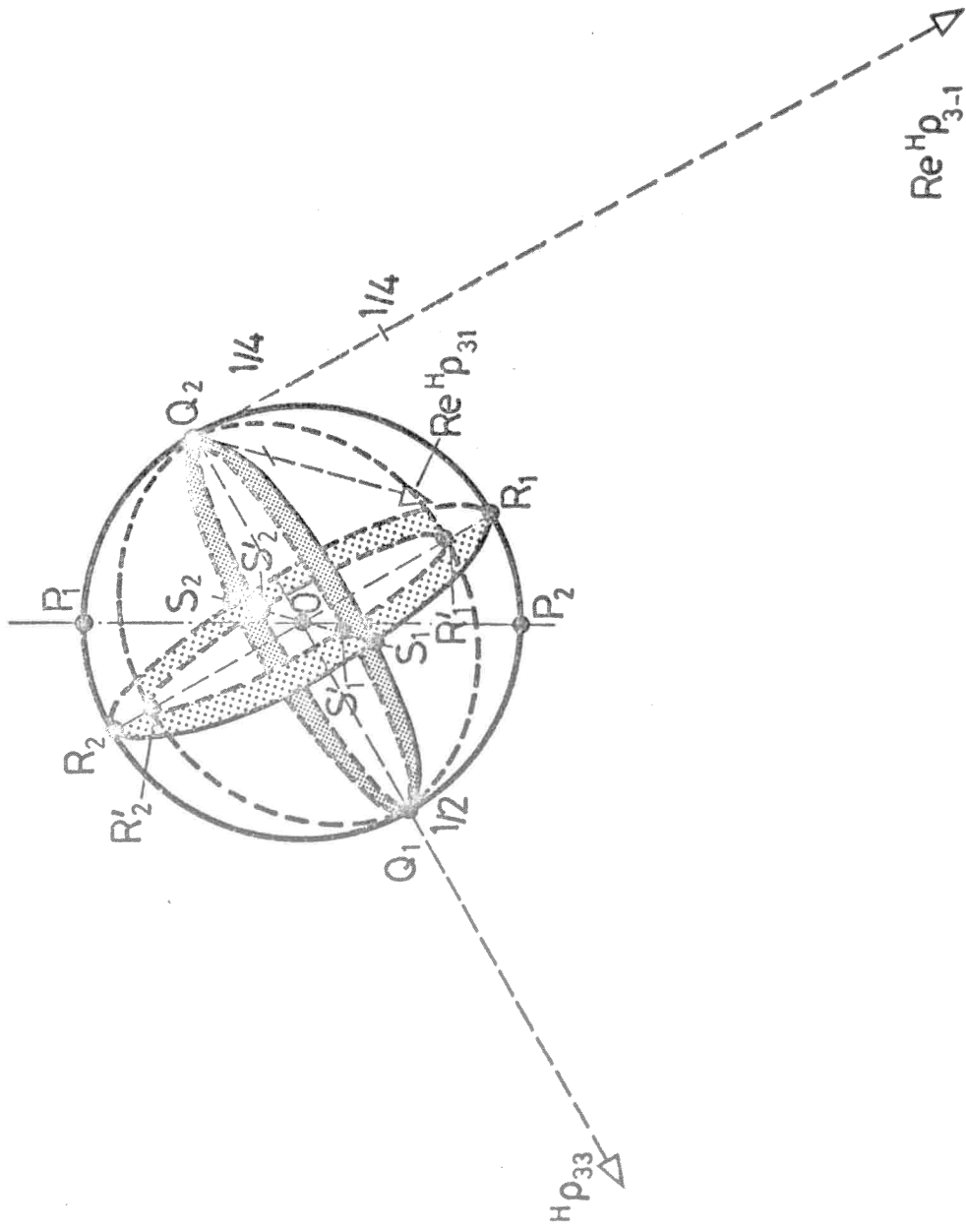


FIG. 3.4

FIG. 3.4 - Polarization subdomain predicted for reactions of type (2) with single trajectory exchange of normal parity in the t -channel. The semi-axes of the ellipsoid are given in (4).

FIGURE CAPTIONS

FIG. 1.1. - Polarization domain for spin $\frac{1}{2}$ particle. a) in the general case (i. e., the whole Poincaré sphere), and b) in the case of B-symmetric production (i. e., the diameter corresponding to polarization along the normal).

FIG. 2.1. - Domain of the even, B-symmetric polarization of spin 1 particle.

FIG. 2.2. - Two-dimensional diagrams for plotting experimental points inside the polarization domain in FIG. 2.1. : a) Meridian section. The plotted point is invariant under frame rotations around the normal. b) Vertical projection. The azimuth of the plotted point is different for s, t, and u frames of quantization.

FIG. 2.3. - Different parametrizations of the polarization domain in FIG. 2.1. : a) Axes of the density matrix elements for any pair of transversity and helicity frames of quantization. b) Deformation of the domain when these transversity axes are normalized. c) Deformation of the domain when these helicity axes are normalized. (The two indicated conical sections are circular).

FIG. 2.4. - Polarization subdomains predicted by t-channel exchange with fixed quantum numbers : $\zeta = P(-1)^J$, $\tau = G(-1)^{J+I}$. The shrinking of these subdomains in the Regge-limit can be estimated by the parameter

$$f = \frac{\overline{P_1 Q_1}}{\overline{P_1 Q}} = \frac{\overline{P_3 Q_3}}{\overline{P_3 Q}}$$

FIG. 2.5. - Values of the Regge-limit parameter f , as function of s and t , for the type (1) reaction $KP \rightarrow K^* P$.

FIG. 2.6. - Values of the Regge-limit parameter f , as function of s and t , for the type (2) reaction $KP \rightarrow K^* N^*$.

FIG. 3.1. - Domain of the even, B-symmetric polarization of spin $\frac{3}{2}$ particle.

FIG. 3.2. - Two-dimensional diagrams for plotting experimental points inside the polarization domain in FIG. 3.1. a) Meridian section. The plotted point is invariant under frame rotations around the normal. b) Vertical projection. The azimuth of the plotted point is different for s, t, and u frames of quantization.

FIG. 3.3. - Different parametrizations of the polarization domain in FIG. 3.1. a) Axes of the density matrix elements for any pair of transversity and helicity frames of quantization. b) Reduction of the domain when these transversity axes are normalized. c) Reduction of the domain when these helicity axes are normalized.

FIG. 3.4. - Polarization subdomain predicted for reactions of type (2) with single trajectory exchange of normal parity in the t-channel. The semi-axes of the ellipsoid are given in (4).